



RESEARCH PAPER

Molecular cloning of the tomato *Hairless* gene implicates actin dynamics in trichome-mediated defense and mechanical properties of stem tissue

Jin-Ho Kang^{1,2,*}, Marcelo L. Campos^{1,‡}, Starla Zemelis-Durfee^{1,3}, Jameel M. Al-Haddad³,
A. Daniel Jones^{4,5}, Frank W. Telewski³, Federica Brandizzi^{1,3} and Gregg A. Howe^{1,5,*}

¹ Department of Energy-Plant Research Laboratory, Michigan State University, East Lansing, MI 48824, USA

² Graduate School of International Agricultural Technology and Crop Biotechnology Institute/GreenBio Science and Technology, Seoul National University, Pyeongchang 25354, Republic of Korea

³ Department of Plant Biology, Michigan State University, East Lansing, MI 48824, USA

⁴ Department of Chemistry, Michigan State University, East Lansing, MI 48824, USA

⁵ Department of Biochemistry and Molecular Biology, Michigan State University, East Lansing, MI 48824, USA

* Correspondence: kangjinho@snu.ac.kr, howeg@msu.edu

‡ Present address: Departamento de Botânica, Instituto de Ciências Biológicas, Universidade de Brasília, 70910-900, Brasília, Distrito Federal, Brazil

Received 24 May 2016; Accepted 9 July 2016

Editor: Christine Raines, University of Essex

Abstract

Trichomes are epidermal structures that provide a first line of defense against arthropod herbivores. The recessive *hairless* (*hl*) mutation in tomato (*Solanum lycopersicum* L.) causes severe distortion of trichomes on all aerial tissues, impairs the accumulation of sesquiterpene and polyphenolic compounds in glandular trichomes, and compromises resistance to the specialist herbivore *Manduca sexta*. Here, we demonstrate that the tomato *Hl* gene encodes a subunit (*SRA1*) of the highly conserved WAVE regulatory complex that controls nucleation of actin filaments in a wide range of eukaryotic cells. The tomato *SRA1* gene spans a 42-kb region containing both *Solyc11g013280* and *Solyc11g013290*. The *hl* mutation corresponds to a complex 3-kb deletion that removes the last exon of the gene. Expression of a wild-type *SRA1* cDNA in the *hl* mutant background restored normal trichome development, accumulation of glandular trichome-derived metabolites, and resistance to insect herbivory. These findings establish a role for *SRA1* in the development of tomato trichomes and also implicate the actin-cytoskeleton network in cytosolic control of specialized metabolism for plant defense. We also show that the brittleness of *hl* mutant stems is associated with altered mechanical and cell morphological properties of stem tissue, and demonstrate that this defect is directly linked to the mutation in *SRA1*.

Key words: Actin-cytoskeleton network, cell wall, mechanical properties, plant-insect interaction, specialized metabolism, terpenoid, tomato (*Solanum lycopersicum*), trichome.

Introduction

Trichomes are epidermal outgrowths that exhibit remarkable morphological variation between plant species. In addition to being either unicellular or multicellular, trichomes are often

distinguished as being nonglandular (simple hairs) or glandular, with the latter involved in the production and secretion of a wide spectrum of specialized metabolites. Trichomes have

been implicated in several physiological functions related to biotic and abiotic stress resilience. For example, trichomes protect plants against a variety of arthropod herbivores that depend on plants as a source of nutrition, prevent water loss and may also provide protection from UV-B radiation (Karabourniotis *et al.*, 1992; Werker, 2000; Kennedy, 2003).

Molecular genetic studies performed in *Arabidopsis* have provided detailed insight into the regulatory pathways that control the development of simple, unicellular trichomes. These studies have identified multi-protein transcriptional complexes that control the differentiation of trichomes from epidermal pavement cells (Hulskamp *et al.*, 1994; Marks, 1997; Ramsay and Glover, 2005; Yang and Ye, 2013). Characterization of trichome distortion mutants has further revealed a role for the actin-cytoskeleton network in trichome branching, cell expansion, and other aspects of cell morphogenesis (Mathur and Chua, 2000; Mathur *et al.*, 2003; Szymanski, 2005). Increasing interest in multicellular glandular trichomes as ‘biofactories’ for the production of specialized metabolites has stimulated efforts to understand developmental and metabolic processes that define these more complex epidermal structures and their role in plant interactions with the environment (Schillmiller *et al.*, 2008; Bergau *et al.*, 2015). The extent to which mechanisms underlying the developmental control of trichomes in *Arabidopsis* applies to multicellular glandular trichomes, however, is largely unknown.

Cultivated tomato (*Solanum lycopersicum* L.) and its wild relatives have several morphologically distinct trichome types, including both non-glandular and glandular structures (Luckwill, 1943). Among the best studied of these are the type I and VI glandular trichomes. Type I trichomes are characterized by a multicellular base, a long (~2 mm) multicellular stalk, and a small glandular tip that secretes acyl sugars (Goffreda *et al.*, 1990; Schillmiller *et al.*, 2012). The type VI trichome has a short (~0.1 mm) stalk and a four-celled glandular head in which high concentrations of terpenoids and flavonoids are produced (Kennedy, 2003; Kang *et al.*, 2010a; Bergau *et al.*, 2015). Recent advances in ‘omics’ technologies have helped to elucidate the biochemical pathways that underlie the production of these compounds (Sallaud *et al.*, 2009; Schillmiller *et al.*, 2009, 2012; McDowell *et al.*, 2011). Complementary genetic approaches have provided evidence for a link between glandular trichome chemistry and resistance of cultivated tomato to arthropod herbivores (Kang *et al.*, 2010a, b; Tian *et al.*, 2012). In only a few cases, however, have genes that are required for proper development and function of glandular trichomes been identified. For example, the *jai-1* mutation defines a component (CORONATINE-INSENSITIVE1) of the jasmonate (JA) receptor whose activity modulates the density and metabolic output of glandular type VI trichomes (Li *et al.*, 2004a; Katsir *et al.*, 2008). It has also been shown that loss-of-function of the flavonoid pathway enzyme chalcone isomerase (CHI1) is associated with reduced density and metabolic output of type VI trichome glands (Rick *et al.*, 1976; Kang *et al.*, 2014). In contrast, downregulation of the methyl-D-erythritol 4-phosphate (MEP) pathway enzyme 1-deoxy-D-xylulose 5-phosphate synthase 2 (DXH2) increases type VI

trichome density (Paetzold *et al.*, 2010). The tomato *Woolly* gene encodes a homeodomain-containing transcription factor that specifically controls the development of type I trichomes (Yang *et al.*, 2011). These collective findings indicate that the development of various trichome types in tomato involves regulatory processes that are specific to a particular structure. A better understanding of trichome development and function could be achieved through the study of genes that affect multiple trichome types in a single plant species.

The *hairless* (*hl*) mutant of tomato was identified more than a half-century ago as a spontaneous mutant that is defective in trichome production on stems and hypocotyls (Rick and Butler, 1956). Reeves (1977) noted that the ‘hairless’ phenotype of the mutant is not caused by the absence of trichomes but rather the development of trichomes that are severely bent and shortened, which imparts a granular appearance to epidermal surfaces (Fig. 1). Subsequent studies showed that *hl* plants are deficient in the accumulation of sesquiterpene and polyphenolic compounds within type VI glandular trichomes and that this metabolic phenotype is associated with decreased resistance to insect herbivory (Kang *et al.*, 2010b). Here, we used a map-based cloning approach to demonstrate that *Hl* encodes the highly conserved SRA1 (specifically Rac1-associated protein) subunit of the WAVE regulatory complex (WRC), which is known to control branching of actin filaments in response to various signal inputs at the cell surface. Transgenic complementation experiments showed that *SRA1*

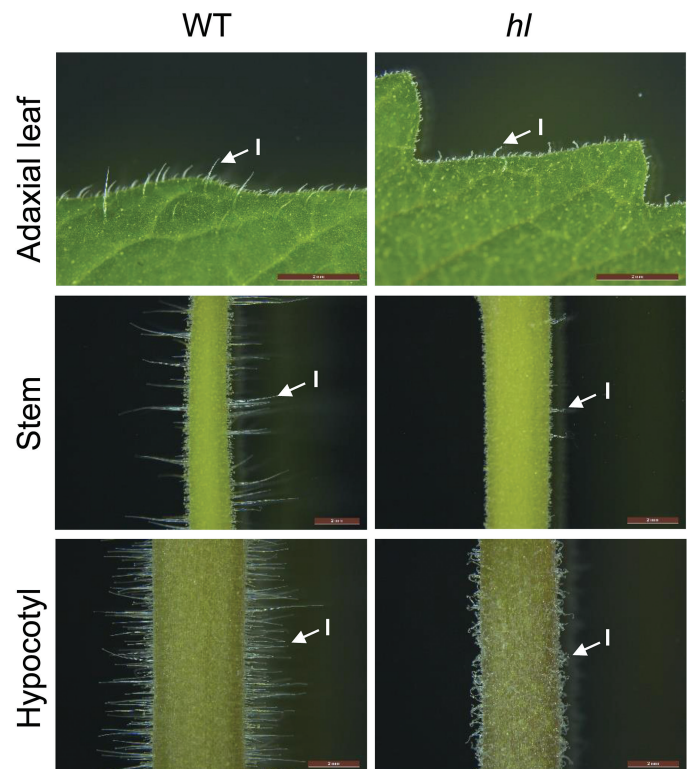


Fig. 1. Light micrographs of trichomes on the leaf, stem, and hypocotyl of WT and *hl* plants. Photographs show the adaxial leaf surface (upper row), stem (middle row), and hypocotyl (lower row) of each genotype. Arrows indicate representative type I trichomes. Scale bar, 2 mm. Three-week-old plants were used for all photographs. (This figure is available in color at *JXB* online.)

is required for normal development of all trichome types, accumulation of flavonoids and sesquiterpenoids in type VI glands, and resistance to *M. sexta*. These findings reveal a function for *SRA1* in glandular trichome development and further suggest that actin-cytoskeleton dynamics play a role in the production of cytosolic metabolites that confer resistance to insect herbivores. We also demonstrate that the *hl* mutation is responsible for the brittleness of mutant stems, thus establishing a role for *SRA1* in mechanical properties of tomato tissues.

Materials and methods

Plant materials and growth conditions

Tomato (*Solanum lycopersicum*) cv Alisa Craig (LA2838A) was used as the wild type (WT) for all experiments. Seeds for WT and *hairless* (*hl*, accession number LA3556) were obtained from CM Rick Tomato Genetics Resource Center (University of California, Davis, USA). Seedlings were grown in Jiffy peat pots (Hummert International, Earth City, MO, USA) in a growth chamber maintained under 17 h of light ($265 \text{ mE m}^{-2} \text{ s}^{-1}$) at 27 °C and 7 h of dark at 18 °C and 60% humidity. Three- to four-week-old plants were sampled for morphological and secondary metabolite analysis.

Genetic mapping of *Hl*

Fine mapping of *Hl* was performed with an F_2 population derived from a cross between *hl* mutant (LA3556) and *S. pennellii* (LA0716), and was facilitated by the tomato genome sequence (Tomato Genome Consortium, 2012). A population of 376 F_2 plants was scored for the distorted trichome phenotype and subsequently genotyped with PCR-based COS (conserved ortholog set) markers (Tomato-EXPEN 2000 map; <https://solgenomics.net>). In some cases, new PCR-based markers were developed by comparing orthologous *S. pennellii* and *S. lycopersicum* EST sequences obtained in the Solanum Trichome Project (<http://www.trichome.msu.edu>). Primer sequences used for mapping are listed in Supplementary Table S1 at JXB online. Genomic DNA extraction and PCR conditions were as previously described (Kang et al., 2010a).

PCR analysis

RNA extracted from leaves (Plant RNeasy Kit, Qiagen) was used for cDNA synthesis (Thermoscript RT-PCR system, Invitrogen) according to the manufacturer's instructions. All primer sets used for reverse transcription (RT)-PCR, including amplification of *SRA1* cDNAs, are listed in Supplementary Table S2. PCR was performed with a DNA Engine Dyad Thermal Cycler (Bio-Rad). RT-PCR reactions (25 μl) contained 15.25 μl H_2O , 2 μl cDNA, 0.75 μl 10 μM solution of each primer, 0.75 μl 10 mM dNTP mix, 5 μl 5 \times KAPA buffer, and 0.5 μl KAPA DNA polymerase (KAPAHiFi HotStart, Kapa Biosystems). The amplification protocol included an initial 5-min denaturation step at 95 °C, followed by 30 cycles in which the template was denatured for 20 s at 98 °C, annealed for 15 s at 65 °C, and extended for 3 min at 72 °C, followed by a final incubation for 5 min at 72 °C. Amplified DNA products were separated on a 1% agarose gel. Amplification of transcripts for eukaryotic Initiation Factor 4A (*eIF4A*) was included as a loading control. 3'RACE (rapid amplification of cDNA ends) was used to determine the polyadenylation sites of *SISRA1* transcripts from WT and *hl* plants.

Genomic DNA fragments corresponding to specific regions of *SISRA1* in WT and *hl* plants were PCR-amplified using the primer sets (gPIR1–gPIR15) listed in Supplementary Table S2. PCR reactions (20 μl) contained 6 μl H_2O , 2 μl genomic DNA template, 1 μl of a 10 μM solution of each primer and 10 μl of Taq polymerase 2 \times

MeanGreen Mastermix (Syzygy Biotech). Amplicons were produced by an initial 5-min denaturation step at 94 °C, followed by 30 cycles in which the template was denatured for 45 s at 94 °C, annealed for 30 s at 52 °C, and extended for 1 min at 72 °C, followed by a final incubation for 10 min at 72 °C. Amplified products were separated on a 1% agarose gel. PCR-amplified fragments were cloned into the pGEM-T-Easy plasmid vector (Promega). Automated nucleotide sequencing was performed at the Michigan State University Genomics Technology Support Facility (<http://rtsf.msu.edu/>).

Transgenic plants

A pGEM-T plasmid containing a cDNA for the entire coding region of *SISRA1* was reamplified with the PIR-SX primer set (Supplementary Table S2). The resulting fragment was digested with *SpeI* and *XhoI* to release a 3.9-kb fragment. This product was cloned into *SpeI* and *XhoI* sites of the pBI-TS binary vector, which contains the Cauliflower Mosaic Virus (CaMV) 35S promoter and nopaline synthase (NOS) terminator (Koo et al., 2006; Schillmiller et al., 2007), to generate pBI-35S:*SRA1*. The resulting construct was introduced into *Agrobacterium tumefaciens* strain EHA105 and used to transform *hl* cotyledon explants as described previously (Li and Howe, 2001; Li et al., 2003). The presence of the T-DNA insert in independent primary (T_0) transformants was confirmed by PCR using the 35S:*SRA1* primer set (Supplementary Table S2) to amplify a fragment spanning the CaMV promoter and *SRA1* cDNA. Regenerated T_0 transgenic plants containing the *SRA1* transgene were potted in soil and transferred to a growth chamber for preliminary analysis of trichome development. These plants were subsequently transferred to a greenhouse for collection of seed (T_1 generation) from individual lines. T_1 seedlings exhibiting normal trichome development were selected from lines in which the ratio of normal:distorted trichomes was $\sim 3:1$. Plants exhibiting normal trichomes were grown in a greenhouse for collection of T_2 -generation seed. Lines in which all T_2 progeny exhibited normal trichomes were selected as being homozygous for the transgene.

Trichome density and morphology

A dissecting microscope (Leica MZ16, Wetzlar, Germany) equipped with KL 2500 LCD light sources (Schott, Jena, Germany) and Leica DFC 290 camera (Leica, Wetzlar, Germany) was used to document trichome morphology and density as previously described (Kang et al., 2010a, b). These measurements were performed with WT, *hl*, and *SRA1*-complemented lines grown together in the same growth chamber.

Metabolite analysis

Leaves from 4-week-old plants were used to prepare type VI trichome exudates and measure flavonoid and terpenoid derivatives as previously described (Kang et al., 2010b). Briefly, a defined number of type VI glands were collected with a stretched Pasteur pipette. For flavonoid analysis, glands were dissolved in 100 μl methanol:acetic acid:water (9:1:10) containing propyl-4-hydroxybenzoate as an internal standard. For terpenoid analysis, glands were dissolved in 100 μl methyl tertiary-butyl ether containing tetradecane as an internal standard. Quantification of metabolites was performed using HPLC/time-of-flight MS for nonvolatile metabolites and GC-MS for volatile terpenes (Kang et al., 2010b).

Insect feeding trials

Tobacco hornworm (*Manduca sexta*) eggs were obtained from Carolina Biological Supply Company (Burlington, NC, USA). Eggs were hatched at 26 °C as recommended by the supplier. Hatched larvae were transferred to leaves of 5-week-old tomato plants, unless otherwise indicated. Challenged plants were maintained in a growth chamber for the duration of the feeding trial, as described in

'Results'. As criteria to establish the first-feeding time, larvae were required to feed continuously at the same feeding site for at least 10 s.

Analysis of stem mechanical properties

Green stems from 3-month-old plants were cut into segments that were more than 14 times longer than their diameters, as required for the bending test (Niklas, 1992; Pruyt *et al.*, 2000; Liu *et al.*, 2012) and in compliance with the testing standard ASTM D143 (1994). The four-point bending test was conducted at room temperature by loading the stem segments to failure using a United® universal testing machine (Model SFM-20, United Calibration Corporation, USA) fitted with a 20 lb load cell (89 Newton) and at a crosshead rate of 30 mm min⁻¹. The span length between the two supported stem ends was 99.1 mm, and the distance between either of the two crosshead loading points and the nearest stem grips was 40.8 mm.

Histology

Stems from 3-month-old plants were collected from a 10–15 cm region close to the apical meristem. Sections were fixed overnight in a mixture of 0.5% glutaraldehyde and 4% paraformaldehyde in 1X phosphate-buffered saline. Samples were dehydrated through a series of graded ethanol washes, cleared with HistoClear II® (Electron Microscopy Sciences, cat# 64111-04), and embedded in paraffin wax according to established protocols (Karlgen *et al.*, 2009). Embedded samples were sectioned with a Leica Microtome and sections were kept on FisherBiotech Probe-On Plus Slides at 42 °C overnight. Sample tissue on the slide was deparaffinized in xylene and brought to 70% ethanol using a graded series. For staining of cell walls, samples were stained with Safranin O and Fast Green using established procedures (Johansen, 1940). Stained slides were sealed in xylene. Iodine staining was performed with tissue samples that were collected, embedded, and sectioned as described above. Sample tissue affixed to a slide was stained with Lugol's iodine solution (6 mM iodine, 43 mM KI, and 0.2 N HCl). Stained samples were viewed with an upright Zeiss AxioImager M2 confocal microscope with settings for bright field. The images were analyzed with AxioVision Rel 4.8 software and assembled with Photoshop Imaging Suite.

Results

Hairless encodes the tomato homolog of *SRA1*

The conspicuous absence of normal type I trichomes on leaves, stems, and hypocotyls of the *hl* mutant (Fig. 1) provided a robust morphological phenotype for fine mapping of the *HL* locus, which was previously mapped to the short arm of chromosome 11 (Rick, 1980; Tanksley *et al.*, 1992). We used an F₂ population derived from a cross between *hl* (LA3556) and *S. pennellii* (LA0716) to refine the map position of *HL* to a ~300-kb region flanked by markers U601668 and T0675 (Fig. 2A). Among the predicted genes in this interval, proteins encoded by two adjacent loci (Solyc11g013280 and Solyc11g013290) were annotated as being homologous to the family of Cytoplasmic FMR1 (Fragile X mental retardation1) interacting proteins (CYFIPs), also known as PIR121 (P53-inducible protein 121) or *SRA1* (Fig. 2B). The CYFIP/PIR121/*SRA1* protein (hereafter referred to as *SRA1*) is a highly conserved component of the heteropentameric WRC that controls actin cytoskeletal dynamics by stimulating the activity of the ubiquitous ARP2/3 complex. In Arabidopsis, mutations in *SRA1* (At5g18410, also known as *KLUNKER*,

PIRP, and *PIROGI*) or other components of the WRC result in distorted trichome phenotypes very similar to those observed in the tomato *hl* mutant (Basu *et al.*, 2004; Brembu *et al.*, 2004; Li *et al.*, 2004b; Saedler *et al.*, 2004). We thus considered Solyc11g013280 and Solyc11g013290 to be strong candidates for *HL*.

Sequence alignments showed that Solyc11g013280 and Solyc11g013290 encode predicted proteins that correspond to the C- and N-terminal regions, respectively, of *SRA1* in Arabidopsis and other species. This observation indicated that Solyc11g013280 and Solyc11g013290 might comprise a single locus. A ~42 kb genomic region encompassing these two loci contains 30 annotated exons that specify a single coding region (Fig. 2B), which has an intron-exon organization that closely matches that of *SRA1* in Arabidopsis. To test whether Solyc11g013280 and Solyc11g013290 comprise a single gene, we performed RT-PCR with wild-type tomato leaf RNA and primers that span the putative ATG start codon in Solyc11g013290 and the TGA stop codon in Solyc11g013280. A single 3.86-kb transcript was amplified and sequenced (Fig. 2C). The cDNA is predicted to encode a 1287 amino-acid polypeptide that shares 81% identity with At*SRA1* (Supplementary Fig. S1). These findings show that Solyc11g013280 and Solyc11g013290 encode a single gene that corresponds to the tomato homolog of *SRA1*.

RT-PCR reactions performed with the same *S/SRA1* cDNA primer set and RNA from *hl* leaves failed to amplify a product (Fig. 2C). Sequencing of the entire 42-kb genomic region of *SRA1* in WT and *hl* plants showed that the mutant harbors a ~3-kb deletion encompassing the entire last (30th) exon within the coding region of the gene, a portion of the preceding intron, and the 3'-untranslated region of the gene (Fig. 2D). Genomic DNA from *hl* retained interspersed sequences derived from the 3'-UTR of WT DNA, suggesting that the deletion is associated with a more complex DNA rearrangement (Fig. 2D; Supplementary Fig. S2). To confirm the sequencing results and further test whether *SRA1* transcripts are expressed in *hl*, we used 3'RACE to amplify the affected region of the transcript. Sequencing of the resulting PCR product from WT and *hl* confirmed that the mutant produces an *SRA1* transcript that is truncated at the 3' end (Fig. 2E). The mutant form of the transcript is predicted to encode a protein that lacks 63 amino acids at the C-terminus of *SRA1* (Supplementary Fig. S3). These collective results demonstrate that the *hl* mutant harbors a deletion in the *SRA1* gene.

Genetic complementation of the *hl* mutant restores normal trichome development

To determine whether the mutation in *SRA1* causes the distorted trichome phenotype of *hl* plants, we used *Agrobacterium*-mediated transformation to complement the mutant with a cDNA that specifies the entire WT *S/SRA1* coding region, under the control of the 35S promoter of *Cauliflower Mosaic Virus* (CaMV). Preliminary visual observations indicated that among seven independent primary

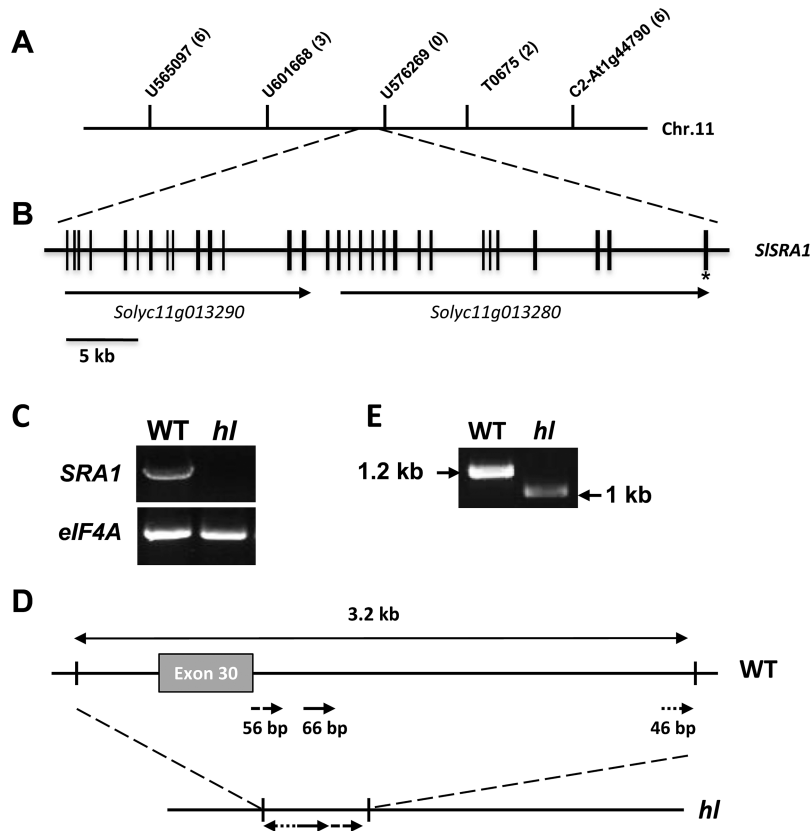


Fig. 2. The *HI* gene encodes the tomato homolog of *SRA1*. (A) Fine genetic mapping of *HI* delimited the target gene to an interval between marker U601668 and T0675 on tomato chromosome 11. Numbers in parentheses indicate the number of recombination events identified between markers and the target gene. (B) Structure of *SISRAl*. Vertical black lines depict exons and horizontal lines indicate intervening introns or intergenic regions. The mutation identified in the *hl* mutant affects the last exon, denoted with an asterisk. The relative location and direction of transcription of annotated genes (*Solyc11g013290* and *Solyc11g013280*) is shown. (C) Agarose gel showing the results of RT-PCR amplification of *SRA1* cDNAs using mRNA isolated from WT and *hl* leaves. *Elongation factor 4A* (*eIF4A*) mRNA was used as a loading control. (D) Diagram depicting the nature of the deletion mutation identified in the *hl* mutant, as compared to the same genomic region of the WT. The *hl* mutation corresponds to a 3.2-kb deletion spanning the last exon of the gene. Arrows depict the directionality of short segments of DNA that are retained in the mutant. (E) Agarose gel showing the amplification products from 3'RACE of the *SRA1* cDNA, using mRNA isolated from WT and *hl* leaves.

(T_0) transformants obtained, all exhibited normal trichome development on stems and hypocotyls (data not shown). Two of these lines (*SRA1-2* and *SRA1-10*) segregated ~3:1 for the normal vs. distorted trichome phenotypes in the T_1 generation and were selected for identification of corresponding T_2 lines that are homozygous for the *35S:SRA1* transgene; these lines were used for all subsequent analyses. Light microscopy showed that the distorted trichome morphology on leaves, stems, and hypocotyls of the *hl* mutant was complemented by the *35S:SRA1* transgene in the *SRA1-2* and *SRA1-10* lines, which were indistinguishable from WT plants at this level of morphological analysis (Fig. 3). We also investigated the potential contribution of *SRA1* to trichome density, as it was previously reported that *hl* leaves have a modest reduction in the density of glandular trichomes (Kang *et al.* 2010b). We confirmed that the density of type VI trichomes on *hl* leaves was significantly less than that of WT leaves at the same developmental stage, and also found that this phenotype was complemented in the *SRA1-2* and *SRA1-10* transgenic lines (Supplementary Fig. S4). These data indicate that the defects in trichome morphology in the *hl* mutant result from a defective *SRA1* gene.

SRA1 modulates the production of trichome-borne metabolites and enhances resistance to insect herbivores

Previous studies showed that type VI glands on the *hl* mutant are deficient in the accumulation of various terpenoid and flavonoid derivatives that are implicated in plant anti-insect defense (Kang *et al.*, 2010b). To test the potential role of *SRA1* in the production of these compounds, we compared the level of terpenoids and flavonoids in type VI glands from WT, *hl*, and the two *SRA1*-complemented transgenic lines. Consistent with previous results, we found that isolated type VI glands from *hl* plants have significantly reduced levels of sesquiterpenes, whereas the monoterpene content in the mutant is unaffected (Fig. 4). The deficiency in sesquiterpene production in *hl* glands was fully complemented in both the *SRA1-2* and *SRA1-10* lines (Fig. 4). We also found that the reduced capacity of type VI glands from *hl* leaves to produce rutin and quercetin trisaccharide was restored to WT levels in the *SRA1-2* and *SRA1-10* plants (Fig. 5). These results establish a role for *SRA1* in the production of sesquiterpene and flavonoid derivatives in type VI glandular trichomes.

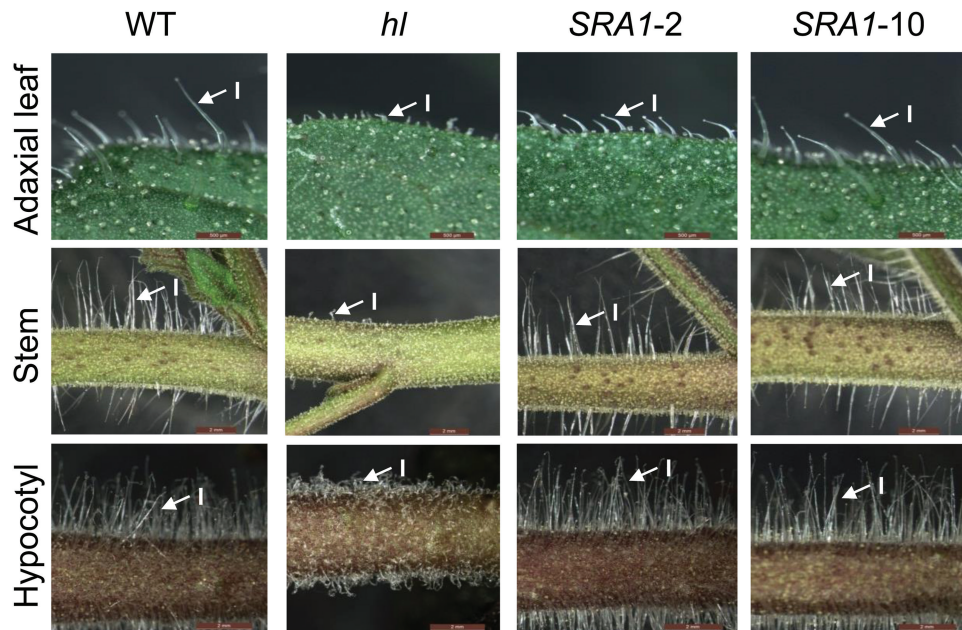


Fig. 3. *SRA1* complements the trichome morphology defect of the *hl* mutant. Light microscopy was used to assess the trichome morphology of WT, *hl*, and two complemented transgenic lines (*SRA1-2* and *SRA1-10*). Photographs show the adaxial leaf surface (upper row), stem (middle row), and hypocotyl (lower row) of each genotype. Arrows indicate representative type I trichomes. Scale bars: 500 μ m, adaxial leaf surface; 2 mm, stems and hypocotyls. Three-week-old plants were used for all photographs. (This figure is available in color at *JXB* online.)

The effect of *hl* on the morphology and chemical composition of leaf trichomes suggested that the mutation might be responsible for the increased susceptibility of the mutant to insect herbivores. To address this question, WT, *hl*, and *SRA1*-complemented plants were challenged with newly hatched *M. sexta* larvae. Insect behavior and time-to-first feeding were observed immediately after the challenge. In comparison to insects on WT plants, larvae that were placed onto *hl* leaves took significantly less time to begin feeding on the leaf lamina (Fig. 6A). Observation of larval behavior suggested that this effect resulted, at least in part, from the presence of type I trichomes that initially impeded the ability of larvae to access feeding sites on the leaf lamina. The feeding behavior of insect larvae on the *SRA1*-complemented lines was indistinguishable from that of insects on WT plants. Following 8 d of continuous feeding, larvae grown on *hl* plants were significantly heavier than those reared on either WT or the transgenic complemented lines (Fig. 6B). These results demonstrate that *SRA1* enhances the resistance of tomato to insect herbivores.

SRA1 affects the mechanical and cell anatomical properties of stem tissue

In addition to effects on trichome morphology, *hl* was previously described as having brittle stems (Butler, 1952; Dempsey and Sherif, 1987). In preliminary experiments we confirmed this trait by observing the behavior of hand-bent stem segments. Bending of WT stems invariably resulted in buckling but not breaking or snapping of the stem (Supplementary Video S1). In contrast, bending of *hl* stems caused the tissue to snap rather than buckle (Supplementary Video S2). Tests performed with *SRA1-2* and *SRA1-10* showed that

stems from these lines, like that of WT, buckled but did not break or snap (Supplementary Videos S3, S4). Next, we conducted four-point bending tests to quantify the contribution of *SRA1* to the material properties of stem tissue. WT stems showed a typical response curve of a ductile composite material while lacking a distinct point of failure (Fig. 7A). However, the response of *hl* stems was characterized by an instant and complete stem failure, reminiscent of brittle materials (Fig. 7B). Loading curves obtained for both *SRA1*-complemented lines were also similar to WT plants (Fig. 7C, D). No significant differences in the elastic modulus were observed between the WT, *hl* and *SRA1*-complemented lines. However, a significant reduction in stem strength (modulus of rupture) was observed in the *hl* line compared to WT, and this reduction in strength was restored in the *SRA1*-complemented lines (data not shown). These results indicate that the brittleness and reduced strength of *hl* mutant results from a defect in the *SRA1* gene.

To determine whether the brittleness of *hl* stems is associated with changes in cell and tissue anatomy, we performed histological analyses to identify lignin-rich and cellulose-rich regions of the stem. The morphology of vascular bundle and pith cells was very similar between WT and *hl* stems (Fig. 8A). Pith cells of *hl* stems, however, were characterized by the presence of granular material that was much less conspicuous in stem sections from WT and the *SRA1*-complemented lines (Fig. 8A). Positive staining of these granules with iodine suggested the presence of starch or related compounds (Supplementary Fig. S5). We also found that the secondary cell walls of bast fiber cells of *hl* mutant were significantly thicker than those of WT and the complemented lines (Fig. 8B, C). These results indicate that defects in *SRA1* expression affect cell homeostasis and stem tensile strength.

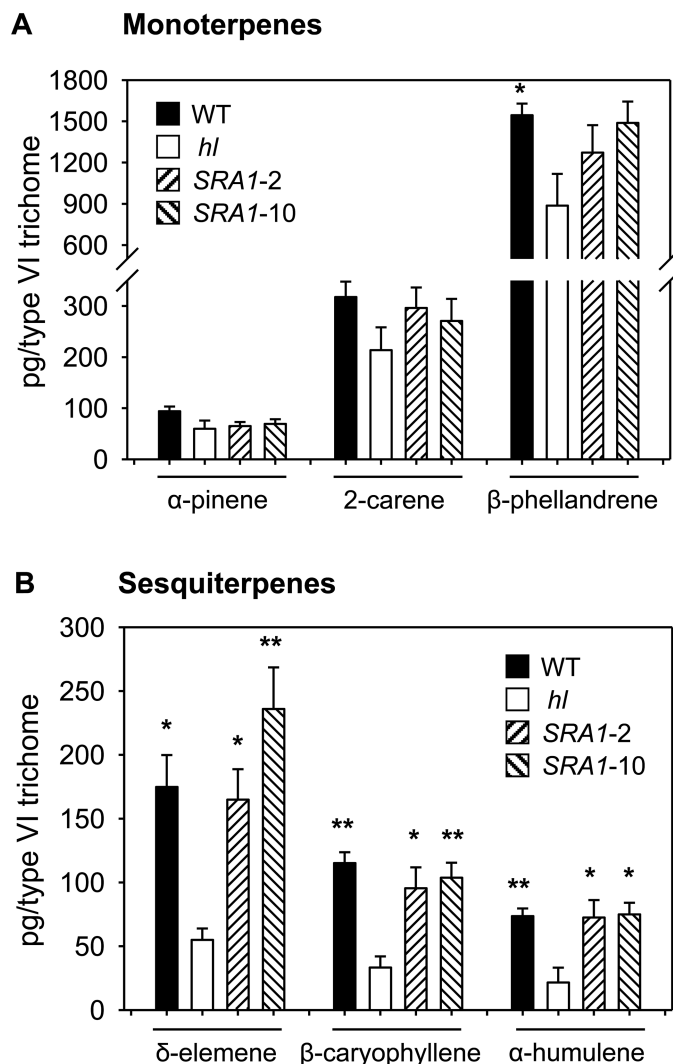


Fig. 4. Mutation of *SRA1* affects terpenoid accumulation in type VI glands. Levels of monoterpenes (A) and sesquiterpenes (B) were measured in type VI glands isolated from leaves of WT, *hl*, and *SRA1*-complemented lines. Peak areas for each compound were normalized on a per gland basis. Each data point represents the mean \pm SE of three or four independent plants per line. Asterisks represent significant differences between *hl* and other genotypes (unpaired *t*-test: *, $P < 0.05$; **, $P < 0.01$).

Discussion

Hl encodes the tomato homolog of *SRA1*

Mutational analysis of unicellular trichome development in *Arabidopsis* has been instrumental for deciphering mechanisms of plant cell fate determination and differentiation. Experimental studies with actin inhibitors and the ‘distorted group’ of trichome mutants have been particularly useful in establishing a role for actin filament organization in polarized cell growth and cell shape (Hulskamp *et al.*, 1994; Mathur *et al.*, 1999; Szymanski *et al.*, 1999; Yanagisawa *et al.*, 2013). Molecular studies have revealed that genes defined by a subset of trichome distortion mutants encode subunits of the ARP2/3 actin filament nucleation complex, as well as components of the WRC that controls the actin-nucleating activity of ARP2/3 complexes (Le *et al.*, 2003; El-Assal *et al.*, 2004a, b; Szymanski, 2005). Based on the phenotypic similarity (e.g.

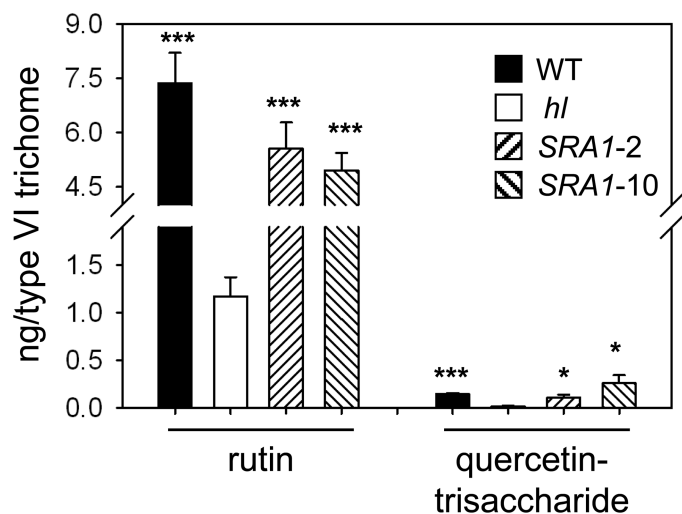


Fig. 5. *SRA1* complements the flavonoid deficiency in type VI trichomes of *hl*. Rutin and quercetin-trisaccharide levels were measured in type VI glands isolated from leaves of WT, *hl*, and *SRA1*-complemented lines. Peak areas for each compound were normalized on a per gland basis. Each data point represents the mean \pm SE of three or four independent plants per line. Asterisks represent significant differences between *hl* and other genotype plants (unpaired *t*-test: *, $P < 0.05$; ***, $P < 0.001$).

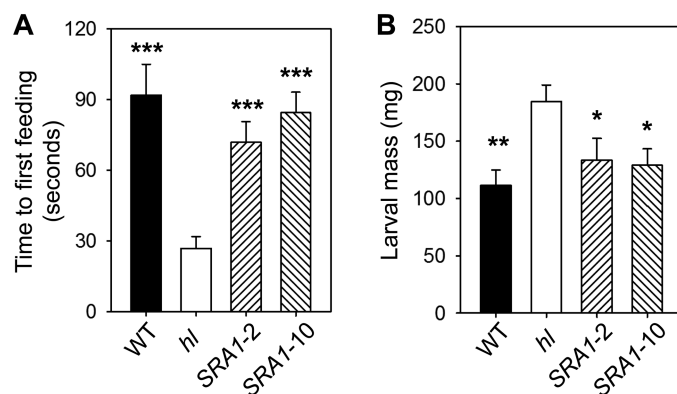


Fig. 6. *SRA1* restores resistance of *hl* plants to feeding by *Manduca sexta* larvae. (A) Newly hatched larvae were placed on the adaxial leaf surface of the indicated genotype, and the time to first feeding on the leaf lamina was measured. Data show the mean (\pm SE) time to first feeding for nine *M. sexta* larvae on leaves of WT, *hl*, and two *SRA1*-complemented lines. (B) No choice bioassays were performed by placing two newly hatched *M. sexta* larvae on leaves of each plant genotype. Data show the mean (\pm SE) mass of larvae ($n=28$) reared for 8 d on the plant. Asterisks represent significant differences between *hl* and other genotypes (unpaired *t*-test: *, $P < 0.05$; **, $P < 0.01$; ***, $P < 0.001$).

severe bending and swelling of trichomes) between these mutants and the tomato *hl* mutant, it was previously suggested that *Hl* might perform a functional role in the actin cytoskeleton network (Kang *et al.*, 2010b). Here, we provide molecular genetic evidence to validate this hypothesis.

Our map-based cloning studies localized the *hl* mutation to the tomato homolog of *SRA1*. In animals, *SRA1* is a subunit of the heteropentameric WRC and is essential for proper control of actin filament assembly (Eden *et al.*, 2002). The WRC is activated by a multitude of signals at the plasma membrane, including kinases, acidic phospholipids, and the small GTPase Rac. Recent studies in both animal and plant

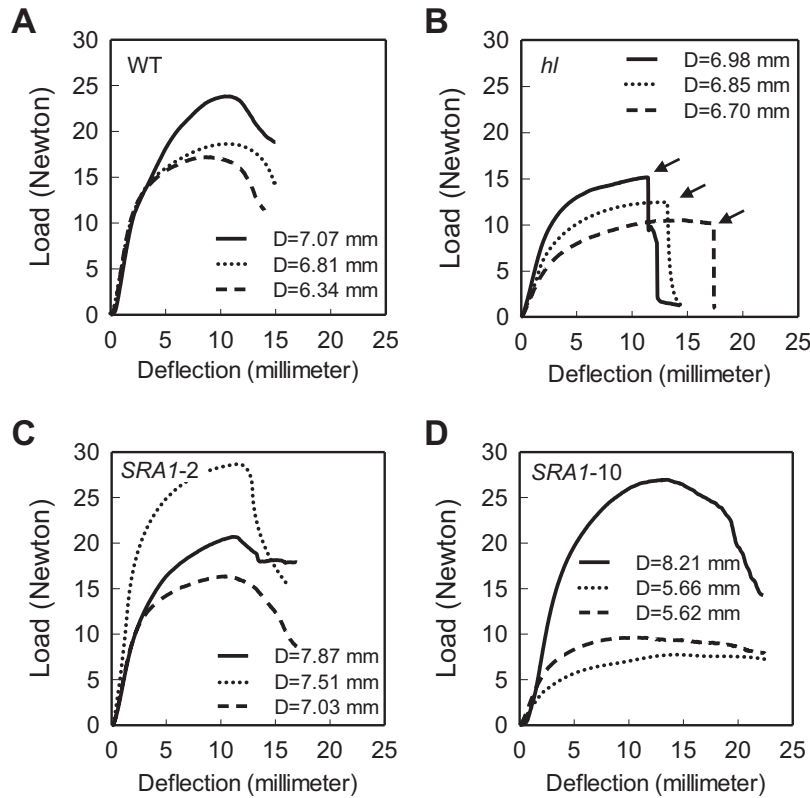


Fig. 7. *SRA1* complements the brittleness of *hl* stem tissue. Stem segments from WT (A), *hl* (B) and two transgenic lines, *SRA1-2* (C) and *SRA1-10* (D), were subject to a four-point bending test as described in ‘Materials and Methods’. The three traces in each panel correspond to the three biological replicates per genotype. The average diameter, *D*, of each stem segment is indicated within the graph. The arrows in panel B indicate the point of complete failure of *hl* stems.

systems have identified receptors that link the WRC to distinct membrane sites, thus establishing a mechanism to promote actin filament assembly in a highly specific, polarized manner (Chen *et al.*, 2014; Facette *et al.*, 2015). The central role of *SRA1* in actin organization is highlighted by its ability to link the WRC, via direct protein-protein interaction, to upstream effectors (e.g. Rac). Given that *sral* mutants of *Arabidopsis* display cell shape and actin-related phenotypes that are very similar to those of ARP2/3 complex mutants, it is generally thought that the WRC promotes ARP2/3 complex activity in plant cells (Mathur *et al.*, 2003; El-Assall *et al.*, 2004a, b; Li *et al.*, 2004b). In support of this view, the *Arabidopsis* and human homologs of *SRA1*, which share ~30% amino acid identity, are functionally interchangeable (Basu *et al.*, 2004).

The trichome distortion phenotype of *hl* plants is similar to that of *sral* null mutations in *Arabidopsis* (Basu *et al.*, 2004; Brembu *et al.*, 2004; Li *et al.*, 2004b; Saedler *et al.*, 2004). Given the established role of *SRA1* in actin dynamics, our results strongly indicate that the trichome morphological phenotypes of the *hl* mutant result from perturbation of the actin-cytoskeleton network. We note, however, that the wide range of developmental and growth phenotypes exhibited by *sral* mutants of *Arabidopsis*, which include leaf epinasty, defects in epidermal cell-cell adhesion, reduced chlorophyll content, and reproductive abnormalities (Li *et al.*, 2004b), are not apparent in the tomato *hl* mutant under our growth conditions (Kang *et al.*, 2010b; this study). These observations raise the question of whether *hl* is a null allele of *SRA1* or

whether the mutant produces a truncated protein that retains partial activity. The *hl* mutation is predicted to generate a C-terminally truncated form of *SRA1* lacking several amino acid residues that are strictly conserved between plants, flies, and humans. Given that we detected truncated *SRA1* transcripts in *hl* tissues, additional studies are needed to more precisely determine how the *hl* mutation affects *SRA1* function.

Role of *SRA1* in trichome chemistry and function

Previously characterized trichome mutants of cultivated tomato, including *af* and *od-2*, have type VI trichomes that are broadly deficient in the accumulation of monoterpenes, sesquiterpenes, and flavonoid derivatives (Kang *et al.*, 2010a, 2014). Interestingly, however, type VI trichomes of the *hl* mutant accumulate monoterpenes but not sesquiterpenes or flavonoids (Kang *et al.*, 2010b; this study). One obvious difference between these broad metabolite classes is their biosynthetic location; whereas monoterpene biosynthesis occurs in plastids, enzymes involved in sesquiterpene and flavonoid production are, in general, located in the cytosol. Our results thus raise the possibility that flavonoid and sesquiterpenoid biosynthesis in the cytosol of glandular trichomes is dependent on the actin-cytoskeleton network. It is conceivable that the cytoskeleton provides a scaffold on which to organize biosynthetic enzymes or facilitate transport of metabolic end products to the vacuole (in the case of flavonoids) or other cellular locations for storage (Widhalm *et al.*, 2015). Indeed, there is considerable evidence

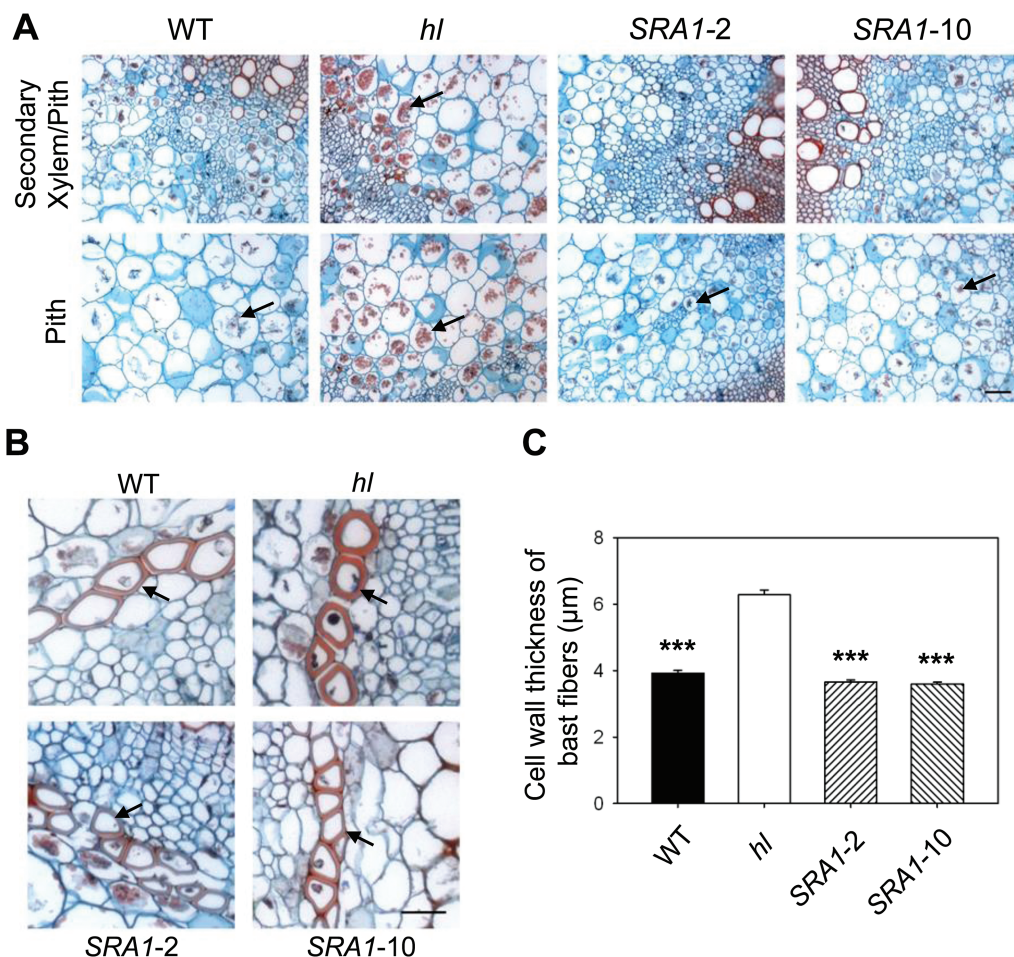


Fig. 8. Mutation of *SRA1* in tomato affects cell anatomy of stem tissue. Cross sections of stem tissue from WT, *hl*, and *SRA1*-complemented lines (*SRA1-2* and *SRA1-10*) were stained with Safranin O and Fast Green. (A) Cells within the secondary xylem and pith regions of *hl* contain red-colored granular structures (arrows) that are less prevalent in WT and *SRA1*-complemented lines. (B) Bast fibers of *hl* stems have thicker cell walls (arrows) than those of WT and *SRA1*-complemented line stems. (C) Quantification of cell wall thickness of bast fibers. Data show the mean (\pm SE) cell wall thickness of at least 60 of bast fibers from three biological replicates per genotype. Asterisks represent significant differences between *hl* and other genotypes (unpaired *t*-test: ***, $P < 0.001$). Scale bars: 100 μ m (A); 50 μ m (B).

implicating the actin cytoskeleton in plant immune responses, including intracellular trafficking of vesicles (Day *et al.*, 2011). Given that *SRA1* also controls translation initiation in animal cells (Schenck *et al.*, 2003; Napoli *et al.*, 2008), we cannot exclude the possibility that changes in chemical composition of *hl* trichomes result from defects in cellular processes other than actin assembly dynamics.

Cultivated tomato uses a multi-layered defense system for protection against a broad spectrum of arthropod herbivores (Howe and Jander, 2008; Peiffer *et al.*, 2009; Campos *et al.*, 2014). Wound- and jasmonate-inducible proteinase inhibitors, amino acid degrading enzymes, and secondary metabolites comprise the dominant chemical defense system within the tomato leaf lamina (Green and Ryan, 1973; Chen *et al.*, 2005, 2006; Gonzales-Vigil *et al.*, 2011). As epidermal structures, trichomes provide constitutive physical and chemical barriers that protect underlying leaf lamina tissues from herbivores. Several lines of evidence indicate that the susceptibility of the *hl* mutant to insect herbivores can be attributed to a defect in trichome-mediated resistance (Kang *et al.*, 2010b; Tian *et al.*, 2012). First, wound-induced production

of leaf proteinase inhibitors is not impaired in the *hl* mutant (Kang *et al.*, 2010b). Second, the *hl* mutant exhibits abnormal trichome development and also accumulates low levels of several trichome-borne metabolites, including flavonoids (e.g. rutin) and sesquiterpenoids, that have been implicated in anti-insect defense (Kennedy, 2003; Kang *et al.*, 2010b). Finally, transgenic complementation studies demonstrate that loss of resistance to the tomato specialist *M. sexta*, as well as defects in trichome morphology and chemistry, is caused by mutation of *SRA1*. Although the results of our insect bioassays clearly show that *SRA1* contributes to host resistance, additional studies are needed to determine the extent to which loss of *SRA1* comprises either physical or chemical aspects of trichome resistance. It is also possible that *hl* impairs the role of glandular trichomes as sensors to detect movement of insect herbivores on the leaf surface (Peiffer *et al.*, 2009).

Role of *SRA1* in mechanical properties of stem tissue

In addition to trichome-related phenotypes, stems of *hl* mutant plants exhibit increased fragility. Dempsey and Sherif (1987)

initially noted that the increased brittleness of *hl* stems is associated with irregularities in phloem fibers of vascular bundles. They also reported that cellulosic microfibrils appear disorganized in the mutant, and that the vesicle content within the cytoplasm is altered as well. Our finding that the *hl* defines a key regulator (SRA1) of actin filament organization provides a new insight into the molecular basis of stem fragility in the mutant. Primary and secondary cell walls have a major impact on the strength and mechanical properties of plant tissues (Niklas and Spatz, 2012). An increasing body of molecular evidence links the cytoskeleton network to various processes involved in the synthesis and deposition of cell wall polymers, which are required for normal cell morphogenesis. Molecular genetic analysis of the *fragile fiber* class of mutants in Arabidopsis, for example, has uncovered several genes involved in the organization of actin and cortical microtubules, including genes required for the trafficking of vesicles that contain cell wall components (Zhong *et al.*, 2004; Bannigan and Baskin, 2005). *fra3* mutations cause a dramatic reduction in secondary wall thickness and a concomitant decrease in stem strength (Zhong *et al.*, 2004). In rice, genetic analysis of the *brittle culm* group of mutants has similarly shown that cell wall synthesis and remodeling are critical for the mechanical strength of tissues (Zhang and Zhou, 2011). Based on the association between the mechanical properties of *hl* stems and altered histological features of vascular bundle and pith cells (Dempsey and Sherif, 1987; this study), it is possible that SRA1 is required for actin cytoskeleton-dependent processes that direct the synthesis or proper deposition of cell wall components, and that disruption of this process in *hl* alters the mechanical properties of stem tissue. It is well established that the WRC responds to upstream input signals to spatially and temporally regulate actin filament assembly to direct vesicle trafficking (Takenawa and Suetsugu, 2007; Yanagisawa *et al.*, 2013). Our results thus provide a foundation on which to better understand how the actin-cytoskeleton network directs the assembly of cell wall polymers that determine mechanical properties of plant tissues.

Supplementary data

Supplementary data are available at *JXB* online.

Table S1. Description of PCR-based mapping markers.

Table S2. Description of PCR primers used in this study.

Figure S1. Amino acid sequence comparison of tomato and Arabidopsis SRA1.

Figure S2. Genomic sequence of the affected region in WT and *hl* plants.

Figure S3. Comparison of the predicted amino acid sequence of SRA1 in WT and *hl* plants.

Figure S4. Density of type VI trichomes on leaves from WT, *hl*, and *SRA1*-complemented transgenic lines.

Figure S5. Iodine staining of pith cells from WT and *hl* stems.

Video S1. Manual bending test of WT stem.

Video S2. Manual bending test of *hl* stem.

Video S3. Manual bending test of *SRA1*-2 stem.

Video S4. Manual bending test of *SRA1*-10 stem.

Acknowledgements

This research was supported by grants from the National Science Foundation (DBI-0604336 and IOS-1456864), the Cooperative Research Program for Agriculture Science & Technology Development (Project No. PJ011841022016), Rural Development Administration, Republic of Korea, the DOE Great Lakes Bioenergy Research Center (DOE BER Office of Science DE-FC02-07ER64494), and AgBioResearch at Michigan State University. We thank Dr Cornelius S. Barry for advice with genetic mapping during the course of the project and Dr Ian Major for assistance with the figures. We acknowledge the MSU Mass Spectrometry and Metabolomics Core for GC-MS resources, the MSU Composite Materials and Structures Center for assistance with materials testing, the CM Rick Tomato Genetics Resource Center (University of California at Davis) for kindly providing tomato seed stocks, and a grant (DE-FG02-91ER20021) from by the Chemical Sciences, Geosciences and Biosciences Division, Office of Basic Energy Sciences, Office of Science, US Department of Energy for infrastructure support and partial support for JHK during the course of this work.

References

- Bannigan A, Baskin TI.** 2005. Directional cell expansion – turning toward actin. *Current Opinion in Plant Biology* **8**, 619–624.
- Basu D, El-Assal SED, Le J, Mallery EL, Szymanski DB.** 2004. Interchangeable functions of Arabidopsis PIPOGI and the human WAVE complex subunit SRA1 during leaf epidermal development. *Development* **131**, 4345–4355.
- Bergau N, Bennewitz S, Syrowatka F, Hause G, Tissier A.** 2015. The development of type VI glandular trichomes in the cultivated tomato *Solanum lycopersicum* and a related wild species *S. habrochaites*. *BMC Plant Biology* **15**, 289.
- Brembu T, Winge P, Seem M, Bones AM.** 2004. *NAPP* and *PIRP* encode subunits of a putative wave regulatory protein complex involved in plant cell morphogenesis. *The Plant Cell* **16**, 2335–2349.
- Butler L.** 1952. The linkage map of the tomato. *Journal of Heredity* **43**, 25–35.
- Campos ML, Kang JH, Howe GA.** 2014. Jasmonate-triggered plant immunity. *Journal of Chemical Ecology* **40**, 657–675.
- Chen BY, Brinkmann K, Chen ZC, Pak CW, Liao YX, Shi SY, Henry L, Grishin NV, Bogdan S, Rosen MK.** 2014. The WAVE regulatory complex links diverse receptors to the actin cytoskeleton. *Cell* **156**, 195–207.
- Chen H, Wilkerson CG, Kuchar JA, Phinney BS, Howe GA.** 2005. Jasmonate-inducible plant enzymes degrade essential amino acids in the herbivore midgut. *Proceedings of the National Academy of Sciences, USA* **102**, 19237–19242.
- Chen H, Jones AD, Howe GA.** 2006. Constitutive activation of the jasmonate signaling pathway enhances the production of secondary metabolites in tomato. *FEBS Letters* **580**, 2540–2546.
- Day B, Henty JL, Porter KJ, Staiger CJ.** 2011. The pathogen-actin connection: a platform for defense signaling in plants. *Annual Review of Phytopathology* **49**, 483–506.
- Dempsey WH, Sherif THI.** 1987. Brittleness in the stem of the seven 'hairless' mutants. *Report of the Tomato Genetics Cooperative* **37**, 4.
- Eden S, Rohatgi R, Podtelejnikov AV, Mann M, Kirschner MW.** 2002. Mechanism of regulation of WAVE1-induced actin nucleation by Rac1 and Nck. *Nature* **418**, 790–793.
- El-Assal SED, Le J, Basu D, Mallery EL, Szymanski DB.** 2004a. Arabidopsis *GNARLED* encodes a NAP125 homolog that positively regulates ARP2/3. *Current Biology* **14**, 1405–1409.
- El-Assal SE, Le J, Basu D, Mallery EL, Szymanski DB.** 2004b. *DISTORTED2* encodes an ARPC2 subunit of the putative Arabidopsis ARP2/3 complex. *The Plant Journal* **38**, 526–538.
- Facette MR, Park Y, Sutimantanapi D, Luo AD, Cartwright HN, Yang B, Bennett EJ, Sylvester AW, Smith LG.** 2015. The SCAR/WAVE complex polarizes PAN receptors and promotes division asymmetry in maize. *Nature Plants* **1**, article number: 14024.
- Goffreda JC, Szymkowiak EJ, Sussex IM, Mutschler MA.** 1990. Chimeric tomato plants show that aphid resistance and triacylglycerol production are epidermal autonomous characters. *The Plant Cell* **2**, 643–649.

- Gonzales-Vigil E, Bianchetti CM, Phillips GN, Howe GA.** 2011. Adaptive evolution of threonine deaminase in plant defense against insect herbivores. *Proceedings of the National Academy of Sciences, USA* **108**, 5897–5902.
- Green TR, Ryan CA.** 1973. Wound-induced proteinase inhibitor in plant leaves: a possible defense mechanism against insects. *Science* **175**, 776–777.
- Howe G, Jander G.** 2008. Plant immunity to insect herbivores. *Annual Review of Plant Biology* **59**, 41–66.
- Hulskamp M, Misra S, Jurgens G.** 1994. Genetic dissection of trichome cell development in *Arabidopsis*. *Cell* **76**, 555–566.
- Johansen D.** 1940. *Plant Microtechnique*. McGraw Hill: London, UK.
- Kang JH, Liu GH, Shi F, Jones AD, Beaudry RM, Howe GA.** 2010a. The tomato *odorless-2* mutant is defective in trichome-based production of diverse specialized metabolites and broad-spectrum resistance to insect herbivores. *Plant Physiology* **154**, 262–272.
- Kang JH, McRoberts J, Shi F, Moreno JE, Jones AD, Howe GA.** 2014. The flavonoid biosynthetic enzyme chalcone isomerase modulates terpenoid production in glandular trichomes of tomato. *Plant Physiology* **164**, 1161–1174.
- Kang JH, Shi F, Jones AD, Marks MD, Howe GA.** 2010b. Distortion of trichome morphology by the *hairless* mutation of tomato affects leaf surface chemistry. *Journal of Experimental Botany* **61**, 1053–1064.
- Karabourniotis G, Papadopoulos K, Papamarkou M, Manetas Y.** 1992. Ultraviolet-B radiation absorbing capacity of leaf hairs. *Physiologia Plantarum* **86**, 414–418.
- Karlgren A, Carlsson J, Gyllenstrand N, Lagercrantz U, Sundstrom JF.** 2009. Non-radioactive *in situ* hybridization protocol applicable for Norway spruce and a range of plant species. *Journal of Visualized Experiments*, e1205.
- Katsir L, Schillmiller AL, Staswick PE, He SY, Howe GA.** 2008. COI1 is a critical component of a receptor for jasmonate and the bacterial virulence factor coronatine. *Proceedings of the National Academy of Sciences, USA* **105**, 7100–7105.
- Kennedy GG.** 2003. Tomato, pests, parasitoids, and predators: Tritrophic interactions involving the genus *Lycopersicon*. *Annual Review of Entomology* **48**, 51–72.
- Koo AJK, Chung HS, Kobayashi Y, Howe GA.** 2006. Identification of a peroxisomal acyl-activating enzyme involved in the biosynthesis of jasmonic acid in *Arabidopsis*. *Journal of Biological Chemistry* **281**, 33511–33520.
- Le J, El-Assal Sel D, Basu D, Saad ME, Szymanski DB.** 2003. Requirements for *Arabidopsis* ATARP2 and ATARP3 during epidermal development. *Current Biology* **13**, 1341–1347.
- Li C, Liu G, Xu C, Lee GI, Bauer P, Ling HQ, Ganai MW, Howe GA.** 2003. The tomato suppressor of prosystemin-mediated responses2 gene encodes a fatty acid desaturase required for the biosynthesis of jasmonic acid and the production of a systemic wound signal for defense gene expression. *The Plant Cell* **15**, 1646–1661.
- Li L, Howe GA.** 2001. Alternative splicing of prosystemin pre-mRNA produces two isoforms that are active as signals in the wound response pathway. *Plant Molecular Biology* **46**, 409–419.
- Li L, Zhao Y, McCaig BC, Wingerd BA, Wang J, Whalon ME, Pichersky E, Howe GA.** 2004a. The tomato homolog of CORONATINE-INSENSITIVE1 is required for the maternal control of seed maturation, jasmonate-signaled defense responses, and glandular trichome development. *The Plant Cell* **16**, 126–143.
- Li Y, Sorefan K, Hemmann G, Bevan MW.** 2004b. *Arabidopsis* NAP and PIR regulate actin-based cell morphogenesis and multiple developmental processes. *Plant Physiology* **136**, 3616–3627.
- Liu Y, Xu F, Gou J, Al-Haddad J, Telewski FW, Bae HJ, Joshi CP.** 2012. Importance of two consecutive methionines at the N-terminus of a cellulose synthase (PtdCesA8A) for normal wood cellulose synthesis in aspen. *Tree Physiology* **32**, 1403–1412.
- Luckwill L.** 1943. *The genus Lycopersicon: historical, biological, and taxonomic survey of the wild and cultivated tomatoes*. Aberdeen University Press: Aberdeen, Scotland.
- Marks MD.** 1997. Molecular genetic analysis of trichome development in *Arabidopsis*. *Annual Review of Plant Physiology and Plant Molecular Biology* **48**, 137–163.
- Mathur J, Chua NH.** 2000. Microtubule stabilization leads to growth reorientation in *Arabidopsis* trichomes. *The Plant Cell* **12**, 465–477.
- Mathur J, Mathur N, Kernebeck B, Hulskamp M.** 2003. Mutations in actin-related proteins 2 and 3 affect cell shape development in *Arabidopsis*. *The Plant Cell* **15**, 1632–1645.
- Mathur J, Spielhofer P, Kost B, Chua N.** 1999. The actin cytoskeleton is required to elaborate and maintain spatial patterning during trichome cell morphogenesis in *Arabidopsis thaliana*. *Development* **126**, 5559–5568.
- McDowell ET, Kapteyn J, Schmidt A, et al.** 2011. Comparative functional genomic analysis of *Solanum* glandular trichome types. *Plant Physiology* **155**, 524–539.
- Napoli I, Mercaldo V, Boyl PP, et al.** 2008. The fragile X syndrome protein represses activity-dependent translation through CYFIP1, a new 4E-BP. *Cell* **134**, 1042–1054.
- Niklas KJ.** 1992. *Plant biomechanics: an engineering approach to plant form and function*. University of Chicago Press: Chicago, USA.
- Niklas KJ, Spatz H-C.** 2012. *Plant Physics*. University of Chicago Press: Chicago, USA.
- Paetzold H, Garms S, Bartram S, et al.** 2010. The isogene 1-deoxy-D-xylulose 5-phosphate synthase 2 controls isoprenoid profiles, precursor pathway allocation, and density of tomato trichomes. *Molecular Plant* **3**, 904–916.
- Peiffer M, Tooker JF, Luthe DS, Felton GW.** 2009. Plants on early alert: glandular trichomes as sensors for insect herbivores. *New Phytologist* **184**, 644–656.
- Pruyn ML, Ewers IB, Telewski FW.** 2000. Thigmomorphogenesis: changes in the morphology and mechanical properties of two *Populus* hybrids in response to mechanical perturbation. *Tree Physiology* **20**, 535–540.
- Ramsay NA, Glover BJ.** 2005. MYB-bHLH-WD40 protein complex and the evolution of cellular diversity. *Trends in Plant Science* **10**, 63–70.
- Reeves AF.** 1977. Tomato trichomes and mutations affecting their development. *American Journal of Botany* **64**, 186–189.
- Rick CM.** 1980. Tomato linkage survey. Report of the Tomato Genetics Cooperative **30**, 2–17.
- Rick CM, Butler L.** 1956. Cytogenetics of the tomato. *Advances in Genetics* **8**, 267–282.
- Rick CM, Quiros CF, Lange WH, Stevens MA.** 1976. Monogenic control of resistance in tomato to tobacco flea beetle: probable repellence by floral volatiles. *Euphytica* **25**, 521–530.
- Saedler R, Zimmermann I, Mutondo M, Hulskamp M.** 2004. The *Arabidopsis* *KLUNKER* gene controls cell shape changes and encodes the ATsRA1 homolog. *Plant Molecular Biology* **56**, 775–782.
- Sallaud C, Rontein D, Onillon S, et al.** 2009. A novel pathway for sesquiterpene biosynthesis from Z,Z-farnesyl pyrophosphate in the wild tomato *Solanum habrochaites*. *The Plant Cell* **21**, 301–317.
- Schenck A, Bardoni B, Langmann C, Harden N, Mandel JL, Giangrande A.** 2003. CYFIP/Sra-1 controls neuronal connectivity in *Drosophila* and links the Rac1 GTPase pathway to the fragile X protein. *Neuron* **38**, 887–898.
- Schillmiller AL, Charbonneau AL, Last RL.** 2012. Identification of a BAHd acetyltransferase that produces protective acyl sugars in tomato trichomes. *Proceedings of the National Academy of Sciences, USA* **109**, 16377–16382.
- Schillmiller AL, Koo AJK, Howe GA.** 2007. Functional diversification of acyl-CoA oxidases in jasmonic acid biosynthesis and action. *Plant Physiology* **143**, 812–824.
- Schillmiller AL, Last RL, Pichersky E.** 2008. Harnessing plant trichome biochemistry for the production of useful compounds. *The Plant Journal* **54**, 702–711.
- Schillmiller AL, Schaubinhold I, Larson M, Xu R, Charbonneau AL, Schmidt A, Wilkerson C, Last RL, Pichersky E.** 2009. Monoterpenes in the glandular trichomes of tomato are synthesized from a neryl diphosphate precursor rather than geranyl diphosphate. *Proceedings of the National Academy of Sciences, USA* **106**, 10865–10870.
- Szymanski DB.** 2005. Breaking the WAVE complex: the point of *Arabidopsis* trichomes. *Current Opinion in Plant Biology* **8**, 103–112.
- Szymanski DB, Marks MD, Wick SM.** 1999. Organized F-actin is essential for normal trichome morphogenesis in *Arabidopsis*. *The Plant Cell* **11**, 2331–2347.

Takenawa T, Suetsugu S. 2007. The WASP-WAVE protein network: connecting the membrane to the cytoskeleton. *Nature Review Molecular and Cellular Biology* **8**, 37–48.

Tanksley SD, Ganai MW, Prince JP, et al. 1992. High-density molecular linkage maps of the tomato and potato genomes. *Genetics* **132**, 1141–1160.

Tian D, Tooker J, Peiffer M, Chung SH, Felton GW. 2012. Role of trichomes in defense against herbivores: comparison of herbivore response to *woolly* and *hairless* trichome mutants in tomato (*Solanum lycopersicum*). *Planta* **236**, 1053–1066.

Tomato Genome Consortium. 2012. The tomato genome sequence provides insights into fleshy fruit evolution. *Nature* **485**, 635–641.

Werker E. 2000. Trichome diversity and development. *Advances in botanical research incorporating advances*. In: *Plant Pathology* **31**, 1–35.

Widhalm JR, Jaini R, Morgan JA, Dudareva N. 2015. Rethinking how volatiles are released from plant cells. *Trends in Plant Science* **20**, 545–550.

Yanagisawa M, Zhang C, Szymanski DB. 2013. ARP2/3-dependent growth in the plant kingdom: SCARs for life. *Frontiers in Plant Science* **4**, 166.

Yang C, Ye Z. 2013. Trichomes as models for studying plant cell differentiation. *Cellular and Molecular Life Sciences* **70**, 1937–1948.

Yang CX, Li HX, Zhang JH, et al. 2011. A regulatory gene induces trichome formation and embryo lethality in tomato. *Proceedings of the National Academy of Sciences, USA* **108**, 11836–11841.

Zhang B, Zhou Y. 2011. Rice brittleness mutants: a way to open the 'black box' of monocot cell wall biosynthesis. *Journal of Integrative Plant Biology* **53**, 136–142.

Zhong RQ, Burk DH, Morrison WH, Ye ZH. 2004. FRAGILE FIBER3, an Arabidopsis gene encoding a type II inositol polyphosphate 5-phosphatase, is required for secondary wall synthesis and actin organization in fiber cells. *The Plant Cell* **16**, 3242–3259.